AGU PUBLICATIONS

JGR

Journal of Geophysical Research: Oceans

RESEARCH ARTICLE

10.1002/2015JC011534

Key Points:
- *Dosidicus gigas* paralarvae of E. Trop. Pacific live above shallow hypoxic layer
- Mesoscale eddies and saline fronts affect paralarvae distribution
- A vertically expanding hypoxic zone may reduce the paralarvae habitat

Correspondence to:
L. Sánchez-Velasco,
lsvelasc@gmail.com

Citation:
Sánchez-Velasco, L., E. D. Ruvalcaba-Aroche, E. Beier, V. M. Godínez, E. D. Barton, N. Díaz-Viloria, and M. R. Pacheco (2016), Paralarvae of the complex *Sthenoteuthis oualaniensis-Dosidicus gigas* (Cephalopoda: Ommastrephidae) in the northern limit of the shallow oxygen minimum zone of the Eastern Tropical Pacific Ocean (April 2012), *J. Geophys. Res. Oceans*, *121*, 1998–2015, doi:10.1002/2015JC011534.

Received 8 DEC 2015
Accepted 10 FEB 2016
Accepted article online 22 FEB 2016
Published online 27 MAR 2016

Paralarvae of the complex *Sthenoteuthis oualaniensis-Dosidicus gigas* (Cephalopoda: Ommastrephidae) in the northern limit of the shallow oxygen minimum zone of the Eastern Tropical Pacific Ocean (April 2012)

Laura Sánchez-Velasco[1], Erick D. Ruvalcaba-Aroche[1], Emilio Beier[2], Victor M. Godínez[3], Eric D. Barton[4], Noe Díaz-Viloria[1], and María R. Pacheco[1]

[1]Departamento de Plancton y Ecología Marina, Centro Interdisciplinario de Ciencias Marinas (CICIMAR-IPN), La Paz, Mexico, [2]CICESE, Unidad La Paz, La Paz, México, [3]Departamento de Oceanografía Física, CICESE, Ensenada, México, [4]Departamento de Oceanografía, Instituto Investigaciones Marinas, Vigo, Spain

Abstract The three-dimensional distribution of the paralarvae of the complex *Sthenoteuthis oualaniensis-Dosidicus gigas* (Cephalopoda: Ommastrephidae) was analyzed at the northern limit of the shallow oxygen minimum zone in the Eastern Tropical Pacific in April 2012. The upper limit of the oxygen minimum water (~44 μmol/kg or 1 mL/L) rises from ~100 m depth in the entrance of the Gulf of California to ~20 m depth off Cabo Corrientes. Most of the paralarvae of this complex, dominated by *D. gigas*, were concentrated in the Gulf entrance, between the thermocline (~20 to ~50 m depth) and the sea surface, in the warmest (>19°C) oxygenated (>176 μmol/kg) layer. The highest abundance of paralarvae was detected in an anticyclonic eddy (~120 km diameter and >500 m deep), which contained lower-salinity water (<35 g/kg), consistent with formation in the California Current. Lower paralarvae abundance was recorded further south off Cabo Corrientes, where hypoxic layers were elevated as water shoaled nearshore. Almost no paralarvae were found in the north of the study area beyond the strong salinity front (~34.8–35.4 g/kg) that bounded the anticyclone. These results showed an affinity of the paralarvae for lower-salinity, oxygenated water, illustrated by the influence of the mesoscale anticyclonic eddy and the salinity front in their distribution. Based on this study, it can be concluded that the expansion of the depth range of hypoxic water observed in the Eastern Tropical Pacific may be increasing environmental stress on the paralarvae by vertically restricting their habitat, and so affecting their survival.

1. Introduction

The jumbo squid, *Dosidicus gigas*, which is the largest ommastrephid squid endemic to the Eastern Tropical Pacific Ocean, is distributed between ~40°N and ~45°S [*Ehrhardt et al*., 1983; *Nigmatullin et al*., 2001]. Found off Peru, Mexico, and California, the highest concentrations support important fisheries with strong impact in the world market [*Argüelles et al*., 2001; *Markaida and Sosa-Nishizaki*, 2001]. The economic importance of the jumbo squid requires improved understanding of ecological aspects of the different phases of its life cycle, and its relation with environment changes on different spatial and temporal scales [*Argüelles et al*., 2001; *Chavez et al*., 2003].

Strong, still unexplained, fluctuations in the size and structure of its population and catch, as well as changes in its distribution, have been documented [*Fiedler et al*., 1992; *Vecchione*, 1999; *Markaida*, 2006; *Robinson et al*., 2015]. A number of studies describe possible relationships between large-scale environmental events and fluctuations in the abundance and distribution of the jumbo squid. The significant expansion of its range, northward from California to as far as Alaska, has been associated with the El Niño of 1997–1998, and the subsequent cool phase has been linked with the latest regime shift in the Eastern Pacific Ocean [e.g., *Chavez et al*., 2003; *Zeidberg and Robison*, 2007; *Bazzino et al*., 2010; *Hoving et al*., 2013]. Other, complementary, studies suggest that the observed changes could be related to the frequency of occurrence of shorter-term phenomena, such as mesoscale fronts and eddies, because most ommastrephids take advantage of these productive areas for feeding, breeding, and spawning [e.g., *Kiyofuji and Saitoh*, 2004; *Gilly et al*., 2006].

The northward expansion of the *D. gigas* populations has also been related with the global expansion of water masses relatively poor in dissolved oxygen [*Stewart et al*., 2013], often called the oxygen minimum zones (OMZs). The OMZs are present in regions of high productivity, where high microbial respiration below the euphotic zone and sluggish deep water mass renewal from midlatitudes and Polar Regions contribute to the formation of steady state low-oxygen zones in the water column [*Gilly et al*., 2013]. There is no consensus on the oxygen threshold defining an OMZ [*Hofmann et al*., 2011], but it has been reported that when oxygen concentrations drop below ~44 μmol/kg or 1 mL/L (denoted here as hypoxic conditions), the pelagic organisms may be stressed. When the oxygen concentrations fall below ~9 μmol/kg (denoted here as suboxic conditions), the organisms may die, as is the case for Atlantic anchovies and some flatfishes, which present mortality between 90 and 100%, at dissolved oxygen concentrations below ~9 μmol/kg [*Gray et al*., 2002; *Diaz and Rosenberg*, 2008; *Stramma et al*., 2008].

The Eastern Tropical Pacific Ocean off Mexico contains the largest naturally hypoxic region of the world [*Fiedler and Talley*, 2006; *Diaz and Rosenberg*, 2008; *Stramma et al*., 2010], but it is one of the least studied in physical and biological terms [*Fernández-Álamo and Färber-Lorda*, 2006; *Davies et al*., 2015]. The northern limit of this OMZ was reported previously by *Cepeda-Morales et al*. [2013], who identify the northern boundary of the shallow OMZ in the Eastern Tropical Pacific off Mexico between 16°N and 23°N. The mean depth of the OMZ (~9 μmol/kg) ranges from 300 to 400 m depth between 20°N and 23°N. Further south (from 16°N to 20°N), the OMZ is much shallower (~60 m depth) because of the poleward transport of hypoxic Subtropical Subsurface Water. The location of the northern limit of the shallow OMZ is associated with the seasonal advection of California Current Water, Subtropical Subsurface Water, and regional mesoscale activity, as has been described by *Godínez et al*. [2010] and *Kurczyn et al*. [2012, 2013].

Possible biological consequences of shallow OMZ expansion [*Stramma et al*., 2008, 2010] include decreased vertical range of the oxygenated habitat for pelagic organisms of all sizes, from zooplankton, including squid paralarvae, to top predators such as the largest ommastrephid squid [*Prince and Goodyear*, 2006; *Gilly et al*., 2006]. Given that the Eastern Tropical Pacific Ocean off Mexico has been reported as one the most important habitats of the jumbo squid, it is evident that changes in the shallow OMZ will have effects on their life cycle. They are particularly sensitive to short-term events during the 2–3 week paralarval stages, but studies of development and vertical migration of the paralarvae in relation to environment are lacking.

Taxonomic studies of the paralarvae of ommastrephid indicate that the paralarvae of the species purple squid *Sthenoteuthis oualaniensis* and *Dosidicus gigas*, species coexisting in this broad region cannot be reliably distinguished by their morphology in the smallest phases (from ~1 to 4 mm in mantle length) and so molecular techniques must be used [*Gilly et al*., 2006; *Ramos-Castillejos et al*., 2010; *Camarillo-Coop et al*., 2011]. When molecular identification is not possible because of formalin preservation or other limitations, paralarvae in the Eastern Tropical Pacific region are generally assigned to the complex *Sthenoteuthis oualaniensis-Dosidicus gigas* "SD complex" [*Vecchione*, 1999; *Staaf et al*., 2013; *De Silva-Dávila et al*., 2015].

The paralarvae of the SD complex have been recorded in the Eastern Tropical Pacific as having their highest abundance in the central region off Mexico during spring and early summer, in agreement with their spawning period in this region [*Ueynagi and Nonaka*, 1993; *Vecchione*, 1999; *Staaf et al*., 2013]. The presence of these paralarvae has also been recorded in the Gulf of California [*Gilly et al*., 2006; *Staaf et al*., 2008; *Camarillo-Coop et al*., 2011; *De Silva-Dávila et al*., 2015] and off the Pacific coast of the Baja California Peninsula [*Ramos-Castillejos et al*., 2010] since the early 1980s. However, in the absence of studies of the vertical distribution of the SD complex in relation to dissolved oxygen, the impact of the expansion of the shallow OMZ on the paralarvae distribution and their survival is unknown. Given the high abundance of paralarvae of the SD complex collected with manta (surface) nets in previous studies in the Eastern Tropical Pacific [*Ueynagi and Nonaka*, 1993; *Vecchione*, 1999; *Staaf et al*., 2013], the oxygenated surface layer is expected to be the preferential habitat of the SD complex. In addition, considering the expansion of the hypoxic and suboxic layers noted by *Diaz and Rosenberg* [2008] and *Stramma et al*. [2010], it might be suggested that the consequent vertical thinning of the oxygenated layer affects the preferred habitat of paralarvae and causes them to expand horizontally to more oxygenated waters. As a contribution to investigating these issues, this study examines the three-dimensional distribution of the paralarvae of the SD complex (Cephalopoda: Ommastrephidae) during its spawning period (April–May) close to the northern limit of the shallow oxygen minimum zone in the Eastern Tropical Pacific Ocean.

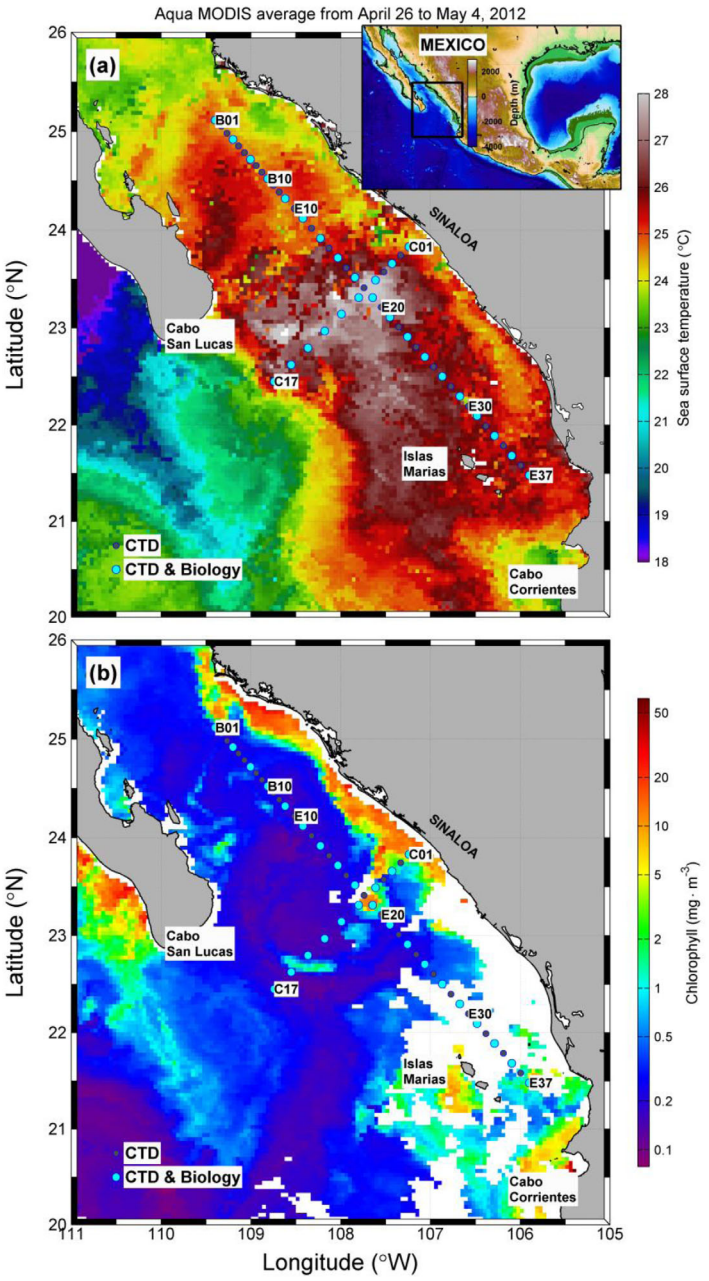

Figure 1. Sampling station locations in the entrance of the Gulf of California (25°N) and Cabo Corrientes (21.5°N) area, in the Eastern Tropical Pacific Ocean off Mexico. Aqua/MODIS (4 × 4 km) satellite images: (a) SST (°C) from 26 April 2012 to 4 May 2012 and (b) Chlorophyll "CHL" (mg/m^3) from 26 April 2012 to 4 May 2012. The symbols indicate Zooplankton and CTD sampling stations (blue circles) and CTD-only sampling stations (dark gray circles).

2. Material and Methods

2.1. Sampling Methods

To obtain a synoptic vision of the ETP off Mexico, satellite images of sea surface temperature (SST) and chlorophyll (4 × 4 km) (CHL) from the Aqua/MODIS satellites were obtained from http://oceancolor.gsfc.nasa.gov/cgi/level3.pl (Figure 1). Geostrophic circulation and mesoscale structures (e.g., eddies) are examined by means of SSHA (Sea Surface height Anomaly). The altimeter data analyzed in this work are the high-resolution sea level anomalies distributed by Ssalto/Duacs at 7 day intervals on a 1/3_Mercator grid, objectively interpolated onto a uniform 1/4_ grid and referenced to a relative 7 year mean (1993–1999) (http://www.aviso.oceanobs.com) [*Ducet et al.*, 2000; *Le Traon et al.*, 2003].

The CTD (Conductivity, Temperature, and Depth) data and zooplankton samples were obtained on board the R/V "Francisco de Ulloa" (CICESE) from 26 April 2012 to 5 May 2012 (Figure 1). One transect (stations B01 to E37 with 41 stations) was made alongshore from the entrance of the Gulf of California to Cabo Corrientes, roughly parallel to the mainland. The second "cross-shore" was perpendicular to the coast from off Sinaloa to the open ocean (C17 to C01 with 11 stations). The transects intersected at station E18 of the alongshore line. The cross-shore line made few days later omitted even number stations after C05 so that the intersection lay midway between C05 and C07. A total of 52 stations were sampled, in which 52 CTD casts and 28 zooplankton tows were taken. The distance between stations along the transect was 10 km. Vertical profiles were obtained at each station using a SeaBird 911plus CTD probe equipped with dissolved oxygen and fluorescence sensors. Conservative Temperature Θ (°C) and Absolute Salinity (S_A, g/kg) were calculated from in situ temperature and practical salinity with the TEOS-10 (Thermodynamic Equation of Seawater-2010) software, which was downloaded from http://www.TEOS-10.org [*IOC et al.*, 2010; *Pawlowicz et al.*, 2010]. Chlorophyll *a* concentration (mg Chl *a*/m^3) was calculated internally by the

fluorometer with the nominal factory calibration, producing a proxy of phytoplankton biomass to be used in relation to physical structures [*Godínez et al*., 2011]. The oxygen dissolved concentration was expressed μmol/kg in accordance with *Hofmann et al*. [2011, 2012]. The CTD data were processed using the calibrations of the manufacturer (http://www.seabird.com/sbe911plus-ctd).

Velocity profiles were measured with a broadband Teledyne-RDI 300 kHz lowered acoustic Doppler current profiler (LADCP) attached to the CTD protection frame. The sampling bins were 8 m thick preprocessed using LDEO IX software [*Thurnherr*, 2010]. The absolute velocity profiles were obtained with the methods described by *Visbeck* [2002]. A standard objective mapping interpolation was applied, using a classic Gaussian correlation function with relative errors of 0.1, a 70 km horizontal length scale and a 30 m vertical scale. The first useful data bin was at approximately 8 m depth.

Vertical distributions of fish larvae are often separable into strata associated with the surface mixing layer, thermocline/chlorophyll *a* maximum layer, and deeper layers [e.g., *Danell-Jiménez et al*., 2009; *Davies et al*., 2015**]**. Given that squid paralarvae of *D. gigas* and *Todarodes pacificus* are demonstrably sensitive to temperature gradients [*Camarillo-Coop et al*., 2011; *Staaf et al*., 2011; *Yoo et al*., 2014], and possibly also to dissolved oxygen **[***Gilly et al*., 2013**]**, net haul sampling was carried out in these three layers. For the purposes of the cruise, the thermocline was defined as the temperature band 16–22°C, which was roughly centered around the maximum temperature gradient. The first stratum was essentially the mixed layer. The second covered the thermocline and the chlorophyll *a* maximum, and the third was from the bottom limit of the hypoxic water (∼9 μmol/kg) to the base of the thermocline/chlorophyll *a* maximum layer, coinciding in most cases with the 44 μmol/kg oxypleth. The depth of each net haul was selected by visual inspection of the CTD profile that preceded each zooplankton tow. The profiles of temperature, chlorophyll *a*, and dissolved oxygen of each station can be found in *Godínez et al*. [2012].

The hauls were performed during day and night using opening-closing conical zooplankton nets with a 60 cm mouth diameter, 250 cm net length, and 505 μm mesh size (http://www.generaloceanics.com). To determine the real depth of each zooplankton tow, the depth of the net was calculated by the cosine of the wire angle method, following the standard procedures of *Smith and Richardson* [1979]. In Table 1, the depth limits and range of each zooplankton tow are shown. In some stations, the real depth range varied significantly from that intended because of changing ambient conditions during the hauls and mechanical problems with the boat winch.

The volume of filtered water was calculated using calibrated flow meters placed in the mouth of each net. Samples were fixed with 5% formalin buffered with sodium borate.

Zooplankton displacement volume, estimated by the displacement volume [*Beers*, 1976; *Kramer et al*., 1972], was standardized to mL/1000 m^3.

Cephalopod paralarvae were separated from the samples, and ommastrephids were identified by morphological characteristics [*Wormuth et al*., 1992]. These paralarvae are known as rhynchoteuthion. Their distinctive form is recognized easily by the presence of a proboscis, which develops into tentacles when the paralarvae reach ∼10 mm of mantle length. When the proboscis suckers were visible, they were checked for correspondence with the genera *Sthenoteuthis* and/or *Dosidicus* (where eight suckers are the same size) [*Gilly et al*., 2006; *Ramos-Castillejos et al*., 2010]. If the proboscis was absent or the suckers were missing, ommastrephids were identified by the characteristic inverted-T funnel locking cartilage of this family. Since all complete organisms found in the samples corresponded to *Sthenoteuthis* and/or *Dosidicus*, all incomplete paralarvae were counted as the same, since other ommastrephids are rare in the Eastern Tropical Pacific [*Staaf et al*., 2013]. Because of the difficulty of identifying paralarvae <4 mm to species level, these were identified as SD complex [*Ramos-Castillejos et al*., 2010; *Staaf et al*., 2013]. Paralarvae >4 mm were identified to species level (*S. oualaniensis* or *D. gigas*) based on the development of ocular and intestinal photophores (present in *S. oualaniensis* and absent in *D. gigas*) [*Ramos-Castillejos et al*., 2010]. The paralarvae abundance was standardized to number of larvae per 1000 m^3.

In order to explore which of the two species dominated the SD-complex, 26 ethanol-preserved paralarvae of this complex (sampling stations E15 and E17) were used to be identified through molecular genetic techniques with a fraction of cytochrome oxidase I (COI) gene of mitochondrial DNA, following the protocols of *Aljanabi and Martinez* [1997], *Gilly et al*. [2006], and *Ramos-Castillejos et al*. [2010]. In molecular genetic

Table 1. Depth Range of Each Zooplankton Tow Sampled Along the Transect Between Gulf of California and Cabo Corrientes (Lines B–E), and the Transect Normal to Sinaloa Coast That Cross the Eddy (line C) in the Eastern Tropical Pacific Ocean Off Mexico

	Mixed Layer Trawl Zooplankton			Thermocline Trawl Zooplankton			Oxygen Minimum Trawl Zooplankton		
Sampling Stations	Initial Depth (m)	Final Depth (m)	Range Layer (m)	Initial Depth (m)	Final Depth (m)	Range Layer (m)	Initial Depth (m)	Final Depth (m)	Range Layer (m)
B01	20	0	20	86	18	67	122	84	38
B04	10	0	10	71	10	61	100	70	30
B07	18	0	18	68	19	49	115	68	48
B10	15	0	15	71	15	56	101	71	30
B13	20	0	20	76	19	58	104	69	35
E11	19	0	19	39	19	19	151	100	51
E13	11	0	11	51	10	41	127	83	44
E15	20	0	20	45	18	27	126	82	44
E17	10	0	10	73	8	64	109	72	37
E19	20	0	20	57	22	35	94	55	39
E21	15	0	15	25	15	10	68	23	45
E23	20	0	20	65	18	47	109	72	37
E25	9	0	9	45	9	36	86	42	44
E27	10	0	10	40	9	31	97	38	59
E29	21	0	21	37	17	20	79	34	45
E31	10	0	10	19	10	10	82	35	47
E33	10	0	10	46	11	35	47	37	10
E35	10	0	10	20	10	10	24	20	4
E37	9	0	9	21	8	13	61	20	40
C01	16	0	16	28	16	13	32	22	10
C03	13	0	13	51	15	36	99	49	50
C05	20	0	20	43	20	23	78	34	45
C07	9	0	9	21	8	12	86	51	35
C09	10	0	10	50	10	40	157	106	51
C11	21	0	21	84	51	33	113	80	33
C13	6	0	6	13	6	7	131	83	47
C15	20	0	20	61	20	41	101	59	42
C17	13	0	13	71	27	44	100	73	27

identification, 11 COI sequences from six *D. gigas* and five *S. oualaeniensis*, from the GenBank, were used as references. Genetic distances of Kimura's two-parameter model [*Kimura*, 1980] among reference sequences of COI and paralarvae sequences were used to display phylogenetic relationships by neighbor-joining (NJ) tree (5000 bootstraps), using MEGA 6.0 software [*Tamura et al*., 2013].

2.2. Statistical Analysis

The nonparametric Kruskal-Wallis test [*Sokal and Rohlf*, 1985; *Siegel and Castellán*, 1988] was used to assess the statistical significance of differences in total paralarval abundance between daytime and nighttime, and among the three depth strata. When the null hypothesis was rejected, a Mann-Witney test was used to establish whether significant differences occurred between pairs of strata [*Daniel*, 2008].

Principal component analysis (PCA) was applied to define the relations between paralarvae distribution of the SD complex and environmental variables. The main matrix of the PCA was the environmental matrix, which contains the zooplankton displacement volume (mL/1000 m^3) of each zooplankton tow where paralarvae were present, and the average of the values of Conservative Temperature Θ (°C), Absolute Salinity (g/kg), chlorophyll *a* (mg Chl *a*/m^3), and dissolved oxygen (μmol/kg) of each zooplankton tow where paralarvae were collected. The standardized abundance of paralarvae was fourth-root transformed, and added as a complementary variable to PCA.

(Θ, S_A) diagrams were constructed in order to investigate relationships between the dissolved oxygen concentrations, the paralarvae abundance, and the water masses during the cruise. The thermohaline boundaries between water masses were graphed as in *Léon-Chávez et al*. [2010, 2015] and *Davies et al*. [2015].

3. Results

3.1. Environmental Variables

Satellite imagery of SST and CHL showed environmental variations between the entrance of the Gulf of California and Cabo Corrientes (Figures 1a and 1b). The sea surface temperature in the cruise area ranged

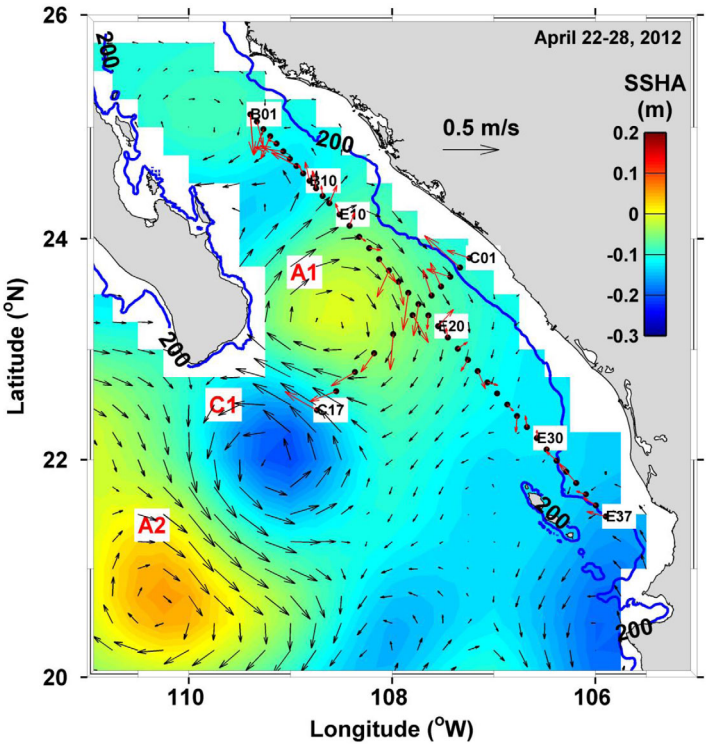

Figure 2. Geostrophic surface velocity vectors and corresponding SSHA (Sea Surface Height Anomaly) derived from AVISO for 22–28 April 2012, between the Gulf of California (25°N) and Cabo Corrientes (21.5°N), in the Eastern Tropical Pacific Ocean off Mexico. A1 and A2, anticyclonic eddies and C1, cyclonic eddy. LADCP velocity vectors averaged over the upper layers, 8–48 m, are shown in red arrows. Blue line, 200 m depth isobath.

between ~24 and 27°C. The highest values were observed in the southern Gulf of California extending in a wide area south of Cabo San Lucas to north of the Las Islas Marias (~24°C), while slightly lower values were seen in upwelling zones along the mainland coast (of Sinaloa) and near Cabo Corrientes (~22°C), and the lowest values (~18°C) were seen in the coastal upwelling off western Baja California, an area outside the ship sampling zone (Figure 1a). The CHL values were low, consistent with oligotrophic conditions in the major part of the study area, except in the upwelling areas along the mainland coast, off Cabo Corrientes, off the western Baja California coast, and around the Islas Marinas, where values reached ~5 mg/m^3 (Figure 1b).

The geostrophic circulation was dominated by three mesoscale eddies of diameter in excess of 100 km, as evident in the gridded SSHA (Figure 2). Relative minima and maxima in sea level indicate cyclonic and anticyclonic circulations, respectively. An anticyclonic eddy A1 (~10 cm SSHA, with velocities ~0.2 m/s) occupied the entrance of the Gulf. Southwest of A1 was a cyclone C1 of similar diameter (−20 cm SSHA, with velocities ~0.3 m/s). Between A1 and C1, a northwestward jet crossed the offshore end of transect C01–C17, while further offshore between C1 and a second anticyclone A2, a jet flowed southeastward from the California Current area. The latter flow coincided with cooler, higher CHL upwelled waters in the images of Figure 1. The area of the eddy A1 corresponded closely with the highest sea surface temperatures and lowest CHL in the satellite data of Figure 1. Transects of sampling stations crossed the eastern and southern peripheries of the anticyclonic eddy A1 (Figure 2). Further to the north, the alongshore transect crossed a weak cyclonic meander inside the Gulf, while south of A1, the circulation was weak close to the sampling line.

LADCP velocity vectors averaged over the upper layers 8–48 m, overlaid in red in Figure 2, show generally good agreement with the surface velocities derived from the altimetry. This is despite the inevitable spatial and temporal blurring caused by the interpolation between altimeter tracks separated in time and space and the instantaneous nature of the LADCP velocities, which contain tidal, inertial, and other high-frequency contributions. One discrepancy occurs at stations C03–C05 near the Sinaloa coast, where the LADCP vectors indicate northward flow opposite to those from altimetry. However, altimetry vectors closest to shore near C01 do agree with the LADCP. It is possible that this difference represents views at slightly different times of the nearshore northward flow known to occur intermittently along this coast [*Lavín et al.*, 2006]. Otherwise, the LADCP vector fields support the location and structure of the eddy A1 as depicted in the altimetry data.

The vertical section of LADCP velocities in the transect B01–E37 (Figures 3a and 3b) showed alternating zones of shoreward and seaward flow with speeds <0.2 m/s. Only the velocity component normal to transect is shown as the along-transect component was relatively uniform. The inshore flank of the eddy A1 detected by satellite was observed between stations B10 and E19, with a width of ~120 km. On the northern side, it had positive (i.e., northeastward) flow with speed >0.05 m/s extending down to ~200 m depth (B10–E12),

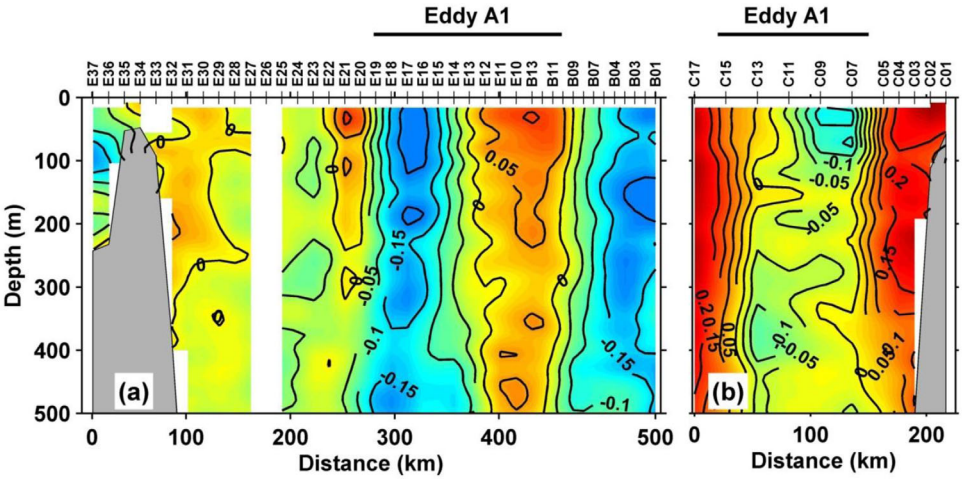

Figure 3. LADCP across-transect velocity component (m/s). (a) The alongshore transect between Gulf of California and Cabo Corrientes (lines B and E) and (b) transect transversal to mainland (line C). The velocity contour interval used is 0.05 m/s. Red colors indicate positive component (northeastward for transect B-E and northwestward for transect C) and blue colors indicate negative components. Black line above the upper abscissa indicates the area of the eddy anticyclonic (A1) that crossed the transects.

and on the southern side, an opposite flow with speeds of >0.15 m/s extending to ~350 m depth (E15–E18). The center of this inshore flank lay between stations E12 and E16. Although velocities weakened with the depth, the same sense of anticyclonic rotation was evident at least to 500 m. The southern periphery of eddy A1 was also sampled in the cross-shore transect C17–C01 between stations C15 and C07. A northwestward component of flow was observed down to at least 500 m at the outer stations (C15–C17), while stations C11–C07 on the inshore flank of the eddy A1 showed a southeastward component.

The vertical Conservative Temperature distributions in Figures 4a and 5a revealed a range from 10 to 28°C in the upper 200 m. The thermocline (here defined as the temperature band 16 to 22°C, roughly centered around the maximum temperature gradient) was found above 50 m depth along the entire transect. Isotherms below 40 m were depressed slightly between stations B12 and E16 at the center of the inshore flank of the eddy A1, and an apparent elevation was observed in those above 40 m near Cabo Corrientes (stations E32–E37). A surface warm pool was observed from near Las Islas Marias to off Cabo Corrientes (from E20 south).

In the cross-shore transect, the thermocline (Figures 4b and 5b) followed the same tendency as in the along-shore transect, except that the depression of the thermocline in the eddy A1 zone, between stations C15 and C07, was more noticeable, probably because this transect crossed closer to the eddy center (Figure 2). The isotherms were elevated near to the Sinaloa coast, corresponding to upwelling seen in Figure 1.

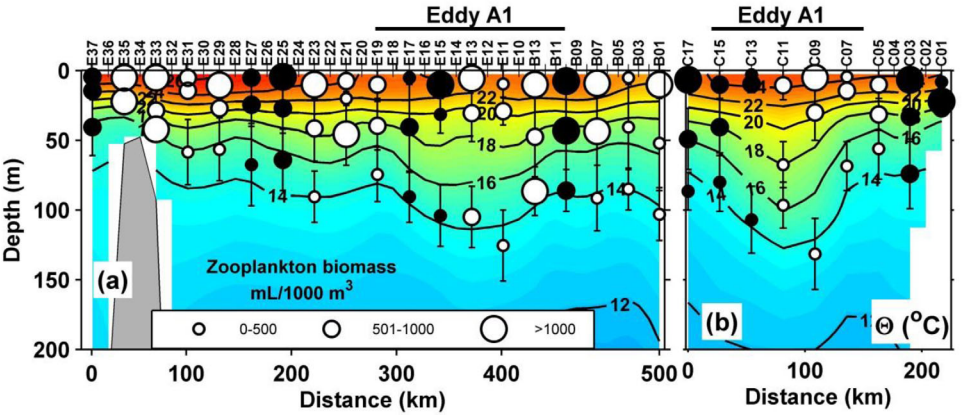

Figure 4. Vertical distribution of zooplankton displacement volume (mL/1000 m^3) and Conservative Temperature Θ (°C) on (a) the alongshore transect between Gulf of California and Cabo Corrientes (lines B and E) and (b) the transect transversal to mainland (line C). The temperature contour interval used was 2°C. Black line above the upper abscissa indicates the area of the eddy anticyclonic (A1) that crossed the transects.

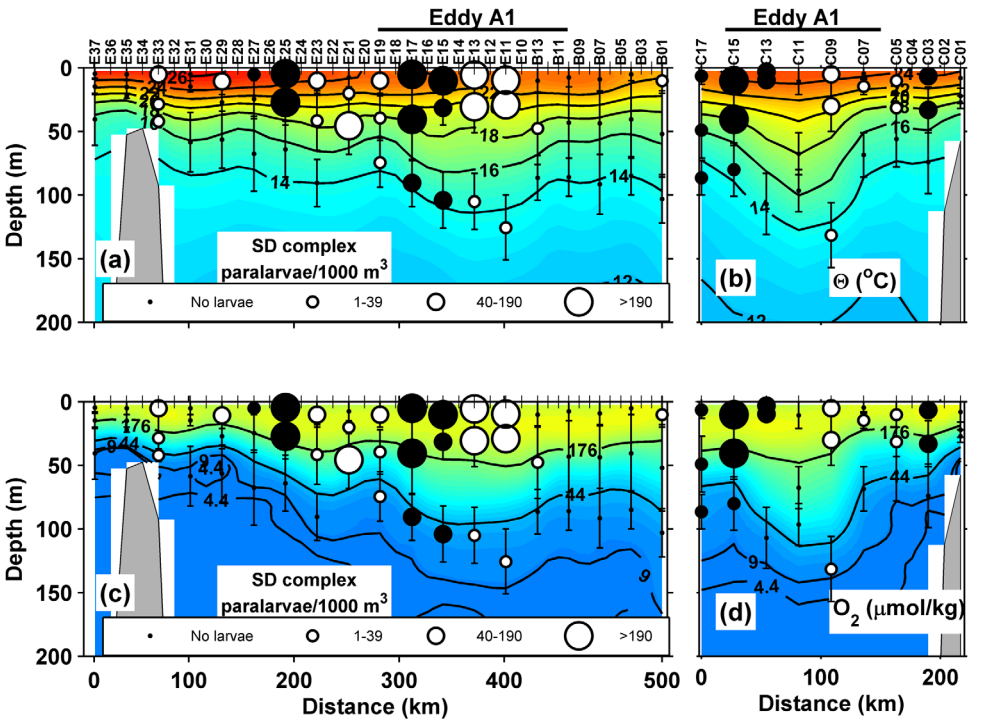

Figure 5. Vertical distribution of the paralarvae of complex *Sthenoteuthis oualaniensis-Dosidicus gigas* and Conservative Temperature (°C) on (a) the alongshore transect between Gulf of California and Cabo Corrientes (lines B and E) and (b) the transect transversal to mainland (line C). The temperature contour interval used was 2 °C. Vertical distribution of paralarvae of SD complex and dissolved oxygen concentration (μmol/kg) on (c) the alongshore transect between Gulf of California and Cabo Corrientes (lines B and E) and (d) the transect transversal to mainland (line C). The isolines of dissolved oxygen showed were 4.4, 9 and 176 μmol/kg. The symbols indicate: day sampling data (white circles) and night sampling data (black circles). Vertical bars show the depth range of each zooplankton haul. Black line above the upper abscissa indicates the area of the eddy anticyclonic (A1) that crossed the transects.

The dissolved oxygen distribution in the transect B01–E37 (Figure 5c) revealed a surface oxygenated layer (>176 μmol/kg) of 30–40 m depth in most of the transect, but thinned to ∼12 m depth near Cabo Corrientes (E37). Values of ($44 < DO < 176$) μmol/kg define the upper limit of the hypoxic water layer, which was situated near 80 m depth in the Gulf of California entrance, deepened slightly between stations B11 and E19 in the center of the inshore flank of the eddy A1, and shoaled to ∼20 m depth near Cabo Corrientes. The upper limit of suboxic waters, indicated by the 9 μmol/kg oxypleth, had a similar overall tendency, rising from ∼180 m depth in the entrance of the Gulf to ∼25 m depth near Cabo Corrientes, showing an appreciable elevation at this cape (between stations E29 and E37) and deepening noticeably in the inshore flank of the eddy A1.

The distribution of the surface oxygenated layer (>176 μmol/kg) along the cross-shore transect C17–C01 **(**Figure 5d**)** is similar to the alongshore transect, showing thinning of the surface layer near to the Sinaloa coast (∼12 m thickness) compared to the ocean side (∼40 m thickness). Both hypoxic and anoxic layers were thinned near to the coast (from station C03 to station C01) as a result of the upwelling showed in Figure 1. In contrast, all the layers deepened significantly where the transect crossed the eddy A1.

The Absolute Salinity ranged between 34.8 and 35.4 g/kg (Figure 6a) showing fluctuations along the alongshore transect parallel to shore in the first 100 m depth. A core of lower salinity (∼34.8 g/kg) was observed between stations E12 and E16, at the center of the eastern flank of eddy A1 (Figure 3a). Salinity fronts were observed to both sides of this salinity minimum, stronger on the Gulf of California side between stations B11 and E11. A surface zone of higher salinity (∼35.2 g/kg) can be seen immediately offshore of Cabo Corrientes (stations E25–E37). Below the more saline surface layers, the salinity was relatively homogenous between 34.9 and 35.1 g/kg down to at least 200 m.

The Absolute Salinity in the transect C17–C01 (Figure 6b) revealed the highest surface salinity values (∼35.2 g/kg) near the Sinaloa coast between stations C07 and C01. The zone near to center of the eddy A1

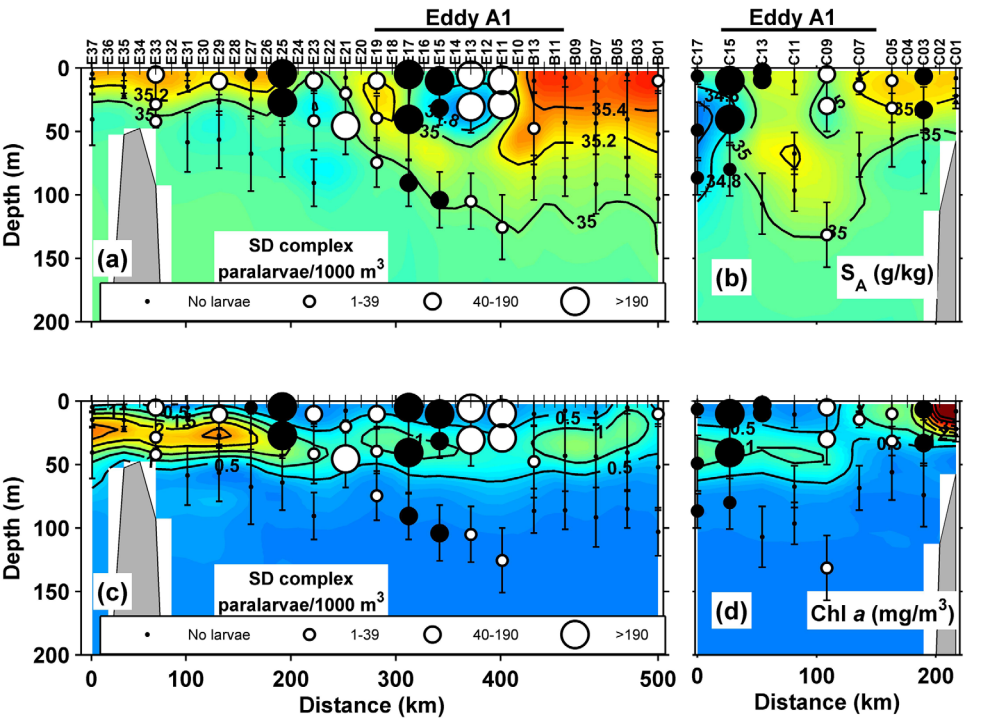

Figure 6. Vertical distribution of the paralarvae of complex *Sthenoteuthis oualaniensis-Dosidicus gigas* and Absolute Salinity (S_A, g/kg) on (a) the alongshore transect between Gulf of California and Cabo Corrientes (lines B and E) and (b) the transect transversal to mainland (line C). The salinity contour interval used was 0.2 g/kg. Vertical distribution of paralarvae of SD complex and chlorophyll *a* (mg/m^3) on (c) the alongshore transect between Gulf of California and Cabo Corrientes (lines B and E) and (d) the transect transversal to mainland (line C). The chlorophyll *a* contour interval used was 0.5 mg/m^3. The symbols indicate: day sampling data (white circles) and night sampling data (black circles). Vertical bars show the depth range of each zooplankton haul. Black line above the upper abscissa indicates the area of the eddy anticyclonic (A1) that crossed the transects.

was marked by deepening of the 35 g/kg isohaline, but the minimum salinity was not as low (<35.0 g/kg) as in the alongshore transect (<34.8 g/kg) and was displaced east of the apparent center (C09). Station C17 also showed water with lower salinities (<34.6 g/kg) between eddies A1 and C1 (Figure 2), likely California Current Water recirculated around the eddy C1.

The chlorophyll *a* values indicated mesotrophic water with maxima of ~2.5 mg/m^3 in both transects (Figures 6 and 7). The chlorophyll *a* concentration was higher in a 45 m thick band in the thermocline (~1–2.5 mg/m^3), with the highest values nearshore, between stations E25 and E37 off Cabo Corrientes and between stations C04 and C01. The isolines of chlorophyll *a*, like the isotherms and oxypleths, showed a slight depression between stations B11 and E18, and C15 and C07, consistent with the presence of the eddy A1. In both transects, the highest values associated with the eddy A1 were found more on its border, rather than nearer to the center.

The zooplankton biomass ranged from 20 to 1100 mL/1000 m^3 showing the highest values (>1000 mL/1000 m^3) in and above the thermocline irrespective of time of day and light conditions in both transects (white fill, light hours; black fill, darkness) (Figures 4a and 4b). In the hypoxic and suboxic water, the zooplankton biomass was lower (<44 μmol/kg) than in the oxygenated layer (>176 μmol/kg).

3.2. Abundance and Three-Dimensional Distribution of Paralarvae

A total of 694 paralarvae were collected in the two transects. Most of them (98%) were of length <4 mm, being classified as SD complex. However, of 28 paralarvae used in molecular genetic identification, all were confirmed to be from *Dosidicus gigas* (Figure 8), showing that the SD complex was dominated by paralarvae of *D. gigas*. The paralarvae >4 mm size were identified as *D. gigas* (10 paralarvae) and *S. oualaniensis* (1 paralarva).

There were no statistically significant differences in the total paralarvae of the SD complex between day and night hours ($P > 0.05$), but there were significant differences among the three strata ($P < 0.05$), with the

Table 2. Paralarvae Abundance Per Sampling Station

Sampling Stations	Mixed Layer Strata (org/1000 m^3)	Thermocline Strata (org/1000 m^3)	Oxygen Minimum Strata (org/1000 m^3)
B01	25	0	0
B04	0	0	0
B07	0	0	0
B10	0	0	0
B13	0	8	0
E11	225	483	10
E13	1517	628	10
E15	5222	76	141
E17	192	197	48
E19	126	16	16
E21	0	34	200[b]
E23	56	33	0
E25	1052	202	0
E27	8	0	0
E29	70	0	0
E31	0	0	0
E33	173	9	16
E35	0	0	0
E37	0	0	0
C01	0	0	0
C03	63	83	0
C05	31	15	0
C07	0	18	0
C09	69	44	9
C11	0	0	0
C13	46	86	0
C15	554	342	6
C17	37	15	7
Mean abundance	338	86	10
Mean Eddy[a] abundance	817	163	26

[a]Considering both transects B13–E19 and C07–C15.
[b]The real range of this trawl was thermocline strata, as shown in Table 1 and Figure 5.

highest abundance in the surface stratum (Table 2). The three-dimensional distribution of the paralarvae of the SD complex (Figures 5 and 6) showed the same pattern during hours of light (white fill) and darkness (black fill) corresponding with the result of the previous test. In both transects, most of the paralarvae were found in the entrance to the Gulf, between the lower limit of the thermocline (~16°C) at ~20–50 m depth and the surface (~26°C) (Figures 5a and b), i.e., in the most oxygenated layer (~176 μmol/kg) of the water column Figures 5c and 5d), coinciding with the layer with the highest chlorophyll a concentrations (Figures 6c and 6d). However, some paralarvae nuclei were observed below this layer, at stations E11 and E19, and at station C09, in the areas influenced by eddy A1, although they were less abundant in the cross-shore transect than in the alongshore transect (Figures 5 and 6).

The highest abundance of the SD complex paralarvae (>100 paralarvae/1000 m^3) were concentrated in the center of the inshore flank of the eddy A1 between stations E11 and E19 of the alongshore transect, where the low-salinity (<35 g/kg) values were observed (Figure 6a and Table 2).

The minimum SD complex paralarvae abundance was recorded off Cabo Corrientes, where bottom depth was shallower and the hypoxic layer was reduced to a thin layer between ~35 and 40 m depth (Figures 5 and 6). Paralarvae were also almost completely absent from the north of the study area, between stations

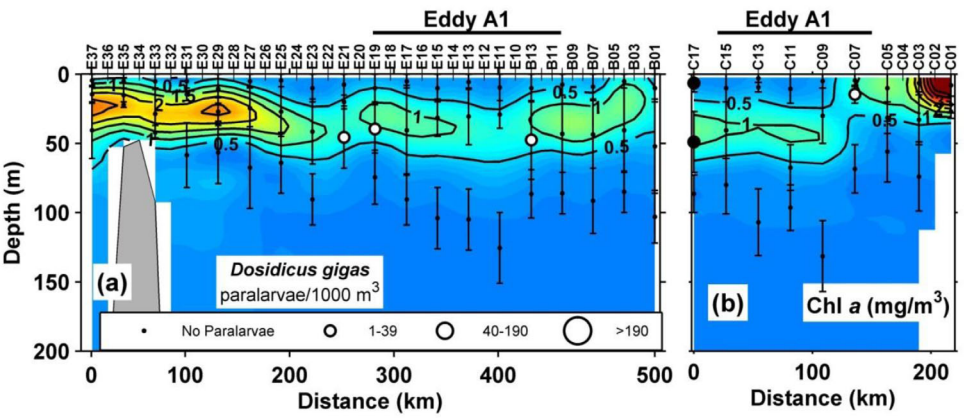

Figure 7. Vertical distribution of paralarvae of *Dosidicus gigas* (paralarvae >4 mm, morphologically identified) and chlorophyll *a* (mg/m^3) on (a) the alongshore transect between Gulf of California and Cabo Corrientes (lines B and E) and (b) the transect transversal to mainland (line C). The chlorophyll *a* contour interval used was 0.5 mg/m^3. Vertical bars show the depth range of each zooplankton haul. Black line above the upper abscissa indicates the area of the eddy anticyclonic (A1) that crossed the transects.

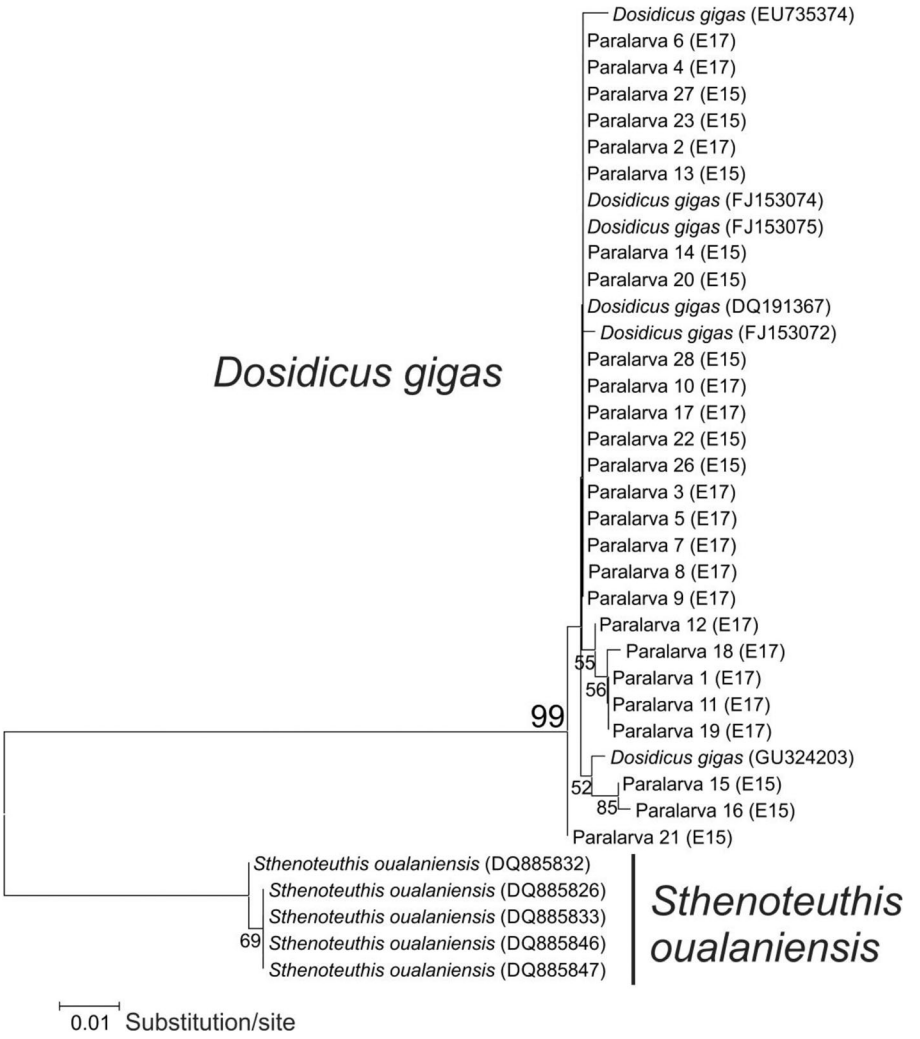

Figure 8. Neighbor-joining tree based on the partial sequences of COI (467 bp) gene of mitochondrial DNA. Numbers beside the branches indicate bootstrap values (>50%), based on 5000 replicates. Accession numbers of references sequences from GenBank and sampling stations of paralarvae are between parentheses. Scale bar represents the genetic distance of Kimura's two parameter.

B01 and B11, beyond the strong salinity front (~34.8–35.4 g/kg) that defined the northern limit of eddy A1 in the entrance of the Gulf (Figure 6).

Even though the number of paralarvae of *D. gigas* of size >4 mm that were identified by morphological characteristics in this work was small (10 paralarvae), these few paralarvae were found in the same layer of the water column as the paralarvae of the SD complex (Figure 7). Most of the *D. gigas* paralarvae were located in salinities >35 g/kg, on the periphery of eddy A1 in both transects, although some were present in station C17, which had salinities < 34.8 g/kg.

The PCA (Figure 9) showed that the abundant data contribute 12% of the total variance, while the first two principal components explained 70% of the total variance in the environmental matrix (Table 3). In a global view, the ordination of the samples indicates that the preferential habitat of the SD complex paralarvae is in the warm, oxygenated water with high chlorophyll *a* and zooplankton biomass. The samples taken in the eddy A1 (filled black circles) were mostly situated in the high-temperature, high oxygen, and low-salinity sector, where the major abundance occurred. Those samples that fell into the right-hand side of the diagram (white circles) were correlated with the hypoxic strata below the eddy A1, but with lower abundances than in the mixed layer and thermocline.

The Θ-S_A diagram corresponding to the temperature range from 5 to 29°C confirmed that the lowest dissolved oxygen concentration corresponded to the temperature range less than 16°C (Figure 10), in the Subtropical Subsurface Water (StSsW) and Pacific Intermediate Water (PIW). The highest dissolved oxygen

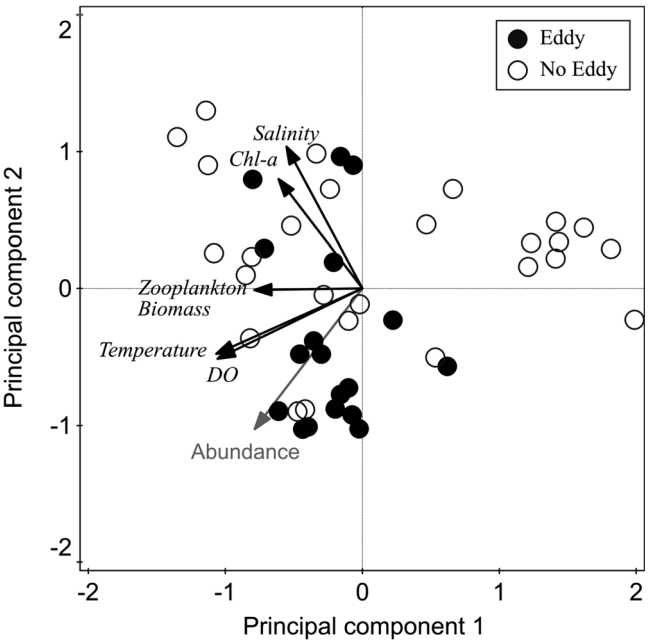

Figure 9. Biplot of Principal Component Analysis, from environmental data and paralarvae of the complex *Sthenoteuthis oualaniensis-Dosidicus gigas* abundance, related to spatial ordination in the Eastern Tropical Pacific Ocean off Mexico, during April 2012.

values were present in surface water masses: Gulf of California Water (GCW) and Transitional California Current-Gulf of California Waters (CCW-GCW) (with thermo-haline characteristics of Tropical Surface Water, but different origin). This last water mass was trapped in the eddy A1 (Figure 6). GCW and CCW-GCW corresponded to temperatures ∼>17°C. Some oxygenated values were observed in California Current Water (CCW) in temperature >15°C.

The Θ-S_A diagram of Figure 10 demonstrates that the SD complex paralarvae were located mostly in the GCW, with high dissolved oxygen, temperature, and salinity (17/40 samples with SD complex presence), and in the CCW-GCW, again with high dissolved oxygen and temperature, but with lower salinity than the GCW (16/18 samples with SD complex presence and high abundance values). The presence of SD complex paralarvae in the California Current Water (CCW) corresponds to paralarvae observed in station C17 at the edge of eddy C1 sampled in the cross-shore transect (Figure 6). The frequency of the SD complex paralarvae was reduced in the StSsW, which was characterized by the hypoxic and suboxic waters (10/25 samples with SD complex presence).

4. Discussion

This work reveals, for the first time, the three-dimensional distribution of paralarvae of the SD complex, most likely composed of *D. gigas*, at the northern limit of the OMZ of the Eastern Tropical Pacific Ocean, the largest natural hypoxic region of the world. It demonstrates the affinity of the paralarvae of the SD complex, for warm (>19°C) and oxygenated (>176 μmol/kg) water. The in situ data illustrate the influence of oceanographic phenomena, such as an anticyclonic eddy or local upwelling, on the distribution of the SD complex (Figures 5 and 6).

4.1. Habitat of the Paralarvae of the SD Complex

The results demonstrate that in spring 2012, the oxygenated layer extended from the sea surface to 30–40 m depth throughout the area, although it thinned slightly off Cabo Corrientes and thickened in the area influenced by the anticyclonic eddy A1 (Figure 5). Similarly, the hypoxic layer (9 >DO >44) μmol/kg was reduced in thickness overall from the entrance of the Gulf of California to off Cabo Corrientes. The oxypleth of ∼9 μmol/kg, rose from a depth of ∼180 m inside the entrance of the Gulf to ∼30 m depth off Cabo Corrientes near the Islas Marias, deepening slightly inside the anticyclonic eddy A1. Thus, the thickness of the

Table 3. Variance Explained by the Principal Component Analysis, From Environmental Data and Paralarvae Abundance, Related to Spatial Ordination in the Eastern Tropical Pacific Ocean Off Mexico, During April 2012

	Axis 1	Axis 2	Axis 3	Axis 4
Eigenvalue	0.781	0.167	0.041	0.010
Variance in Environmental Data				
% of variance explained	78.12	16.73	4.10	1.04
Cumulative % explained	78.12	94.85	98.95	99.99
Pseudocanonical correlation of abundance data	0.576	0.239	0.200	0.263

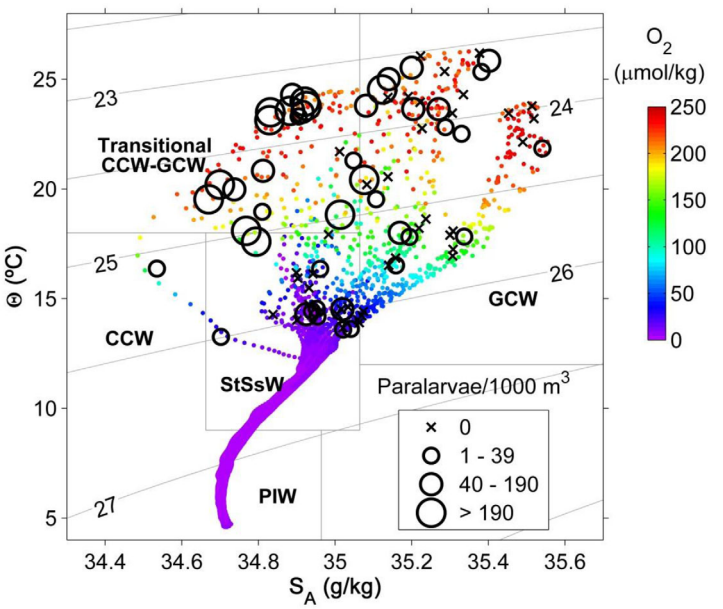

Figure 10. Paralarvae of SD complex distribution (While circles) on the Θ-S_A diagram in the Eastern Tropical Pacific Ocean off Mexico during April 2012. The water masses shown are: California Current Water (CCW), Transitional California Current Water-Gulf of California Water (CCW-GCW), Gulf of California Water (GCW), Subtropical Subsurface Water (StSsW), and Pacific IntermediateWater (PIW). The thermohaline boundaries between water masses are similar to *Léon-Chávez et al*. [2010] and *Davies et al*. [2015]. Density anomalies (gray slanted lines, kg/m^3).

hypoxic layer was reduced overall from ~70 m in the northern area to ~5 m off Cabo Corrientes (Figure 2). These results may be compared with a previous study of a closely similar transect [*Davies et al*., 2015] during winter (mixing period), when the surface oxygenated layer fluctuated between ~40 and 60 m depth, and the hypoxic layer also elevated and thinned toward the south, where it had a thickness of ~40 m depth near Cabo Corrientes. The present study highlights that, with the increased stratification and thinning of the oxygenated and hypoxic layers in spring as compared to winter, suboxic water was introduced to within 50 m of the sea surface, an extreme situation. In both periods, this pattern is influenced by the shoaling near the coast of deeper layers, including those of low oxygen, driven by semicontinuous upwelling off Cabo Corrientes [*Cepeda-Morales et al*., 2013; *León-Cháves et al*., 2015; *Davies et al*., 2015]. These results are in agreement with the climatological maps of the shallow hypoxic layer based on oceanic observations from 1950 to 2002 of *Fiedler and Talley* [2006]; although their shallowest stations are deeper than in this study, both latitudinal (NW to SE) and coastal-oceanic (off Cabo Corrientes) gradients of decrease in the depth of the shallow hypoxic water are clearly observed.

The biological effects of the shallow occurrence of the hypoxic and suboxic layers off Cabo Corrientes, particularly during the stratification period, when the thermocline (~16 to 20°C isotherms) is well established, were difficult to determine because of the scarcity of observations and the sampling strategy. However, if the oxygenated habitat is thinned, it must impact negatively in the survival of zooplankton organisms there, as is the case of the paralarvae of the SD complex. The habitat reduction will cause mortality by increasing environmental stress on the planktonic organisms that are sensitive to minor changes from temperature variations to changes in the trophic niche, such as increase in competition for food [*Lynch*, 1977] and vulnerability to predation, as has been reported for other zooplankton groups [*Clark and Nelson*, 1997; *Rohner et al*., 2013]. There is still little information about the paralarvae habitat, not only in the area of study, but also off the Peru and Chile coasts, where the species also spawns actively [*Argüelles et al*., 2001; *Rosa and Seibel*, 2010].

In this work, most paralarvae of the SD complex, dominated by paralarvae of *D. gigas*, were located in and above the thermocline, in the oxygenated layer corresponding to transitional CCW-GCW and GCW (Figure 10), suggesting that this is the preferential habitat of the paralarvae of the *D. gigas*. *Staaf et al*. [2013], who collected paralarvae with surface (~20 cm depth) and oblique tows (from 200 m depth to surface) in a broad region of the Eastern Tropical Pacific Ocean, found that the highest abundance of paralarvae of SD complex was in the surface tows near temperatures of 29°C. Our study indicates that the paralarvae prefer to dwell in the oxygenated layer above the 16°C isotherm up to the sea surface (~26°C) with strongest affinity to the uppermost layer.

The preference of the paralarvae of the SD complex for the surface layer of the water column contrasts with the reported behavior of the juveniles and adults of these two species coexisting in this region of the

Pacific. The organisms in these pelagic stages, which have been described as active vertical migrators between 1000 m depth and the sea surface, may have an important influence on the vertical energy flow in the pelagic ecosystem and provide an efficient transport of energy from the surface to deeper waters [*Markaida et al*., 2005; *Gilly et al*., 2006]. In fact, *Rosa and Seibel* [2010], in a physiological study of *D. gigas* juveniles, underlined their advantage of greater metabolic efficiency in hypoxic and cold water than other predators. The juveniles and adults thus exhibit a wide range of tolerance for dissolved oxygen concentrations and temperature, contrary to the restricted vertical habitat of their planktonic stages (paralarvae). Nevertheless, the results of *Staaf et al*. [2011] on the role of light on paralarvae behavior, suggest the possibility that the paralarvae may migrate through the thin surface layer on a daily cycle, like fish larvae of coastal demersal species [*Sánchez-Velasco et al*., 2013].

4.2. Paralarvae of the SD Complex and Mesoscale Processes

In the entrance of the Gulf of California, where the hypoxic and suboxic waters were located at greater depth, a strong salinity front associated with the northern boundary of the eddy A1 was detected (Figures 2 and 6). The front resulted from the confluence of the surface water masses of high-salinity GCW ($S > 35.4$ g/kg) with lower-salinity CCW-GCW and the CCW ($S < 34.8$ g/kg) (Figures 6 and 10). Although the data obtained in this study cannot provide a complete description or explanation of the front, the results correspond with previous observations of strong salinity fronts in the entrance to the Gulf of California, where a southward branch of the California Current, called by *Godínez et al*. [2010] the Tropical Branch of the California Current, converges with the poleward Mexican Coastal Current in a constantly shifting zone of complex interaction [*Godínez et al*., 2010; *Kurczyn et al*., 2012; *Collins et al*., 2014; *León-Chávez et al*., 2015].

Biologically, the salinity front might represent the northern limit of the paralarvae distribution in the study (Figure 6) because only two paralarvae were found NW of this front. Even though the salinity front may be a limit for plankton as mentioned in previous studies of fish larvae [*Davies et al*., 2015], adult and juvenile organisms that tolerate broad salinity ranges can enter the Gulf of California in pursuit of better environmental conditions for their planktonic stages, as is the case of the jumbo squid. High abundances of jumbo squid have been reported south of the central archipelago of the Gulf from the early 1980s [*Gilly et al*., 2006; *Staaf et al*., 2008;*Camarillo-Coop et al*., 2011; *De Silva-Dávila et al*., 2015]. However recently, *Robinson et al*. [2015] reported a prolonged decline of jumbo squid landings in the Gulf associated with chronically low wind stress and decreased chlorophyll *a* after El Niño 2009–2010, perhaps reflecting a sensitivity of the adults of the species to major climatic changes. The apparent lack of spawning of *D. gigas*, as indicated by near-zero paralarvae abundance in the south of the Gulf could be related to this decline. However, in this study we have no evidence to substantiate this.

In the present study, the salinity front (~34.6–35.4 g/kg) was associated with the presence of the anticyclonic eddy A1 (~120 km diameter and >500 m depth) (Figures 2, 3 and 6) that contained low salinity of CCW water ($S < 34.8$ g/kg). The altimetry data suggested that water from the California Current region was recirculated around the cyclonic eddy C1 and then around the anticyclonic eddy A1 (Figure 2). However, with only one CTD station showing California Current properties (Figure 10), the sparse sampling does not allow definite conclusions. Future study of the trajectory, extent, and continuity of the surface salinity minimum would clearly contribute to understanding the biological connectivity between the Tropical Branch of the California Current and tropical-subtropical water masses.

The observation that the highest abundance of paralarvae of SD complex, dominated by *D. gigas*, occurred in the eddy A1 in the entrance of the Gulf of California (Figure 6), indicates that mesoscale eddies might affect their distribution, as has been found for other zooplankton groups [*Sánchez-Velasco et al*., 2013; *León-Chávez et al*., 2015]. Previous studies focused on mesoscale eddies in the northeastern tropical-subtropical Pacific Ocean [*Kurczyn et al*., 2012, 2013] indicate continuous generation of mesoscale eddies in this OMZ, with predominance of anticyclonic over cyclonic eddies, as appears general in the ocean [e.g., *Graves et al*., 2006]. It is probable that if the *D. gigas* adults spawn in warm and oxygenated water, in a region where mesoscale eddies occur continuously, the probability for trapping by these would be high. Present results suggest that anticyclones may have an important role in the survival of the planktonic stages of the jumbo squid and other species that inhabitant the region, as well as in modifying the depth of the hypoxic and suboxic waters, with biological implications still unknown.

Anticyclones like the eddy A1 have been studied in various regions to provide a basic understanding of their dynamics, kinematics, and biological effects at regional and mesoscale [e.g., *Aristegui et al*., 1997; *Aristegui and Montero*, 2005; *Sangrà et al*., 2005, 2009; *Baltar et al*., 2009; *Chaigneau et al*., 2011]. However, recent work indicates the importance of submesoscale structures and related vertical mechanisms that are thought to operate [*Klein and Lapeyre*, 2009], such as ageostrophic secondary circulation and mixing, which can modulate the plankton community distribution/structure through localized vertical fluxes. These may be related to the time evolution of eddies [*McGillicuddy et al*., 1998], to eddy/wind interactions in the eddy interior [*Martin and Richards*, 2001; *McGillicuddy et al*., 2007], or to nonlinear Ekman and frontal effects at the eddy periphery [*Mahadevan et al*., 2008]. Such processes may affect different areas of the eddy to produce vertical circulations counter to the accepted idea of general surface convergence leading to sinking at the anticyclone center, and could be responsible for the enhanced chlorophyll *a* concentrations observed in the periphery of A1. However, much more detailed observations and modeling will be required to fully understand the interaction of the paralarvae and other planktonic organisms with the eddy dynamics.

4.3. Final Considerations

Considering the evidence shown in this study, it can be suggested that if the hypoxic water is expanding vertically in this region, as has been documented globally for all OMZs in other environmental research [*Stramma et al*., 2008; *Bazzino et al*., 2010], then the paralarvae habitat of the SD complex, specifically of *D. gigas*, is being reduced into a thinner surface layer. By increasing environmental stress, this may affect paralarvae survival. The thinning of the warm oxygenated layer preferred by the paralarvae by itself might not explain northward expansion of the area of distribution, even if it causes lower abundance locally. However, because thinning is associated with a general warming due to global change, and possibly regime shift in the Eastern Pacific Ocean (a cold phase since 1997) [*Chavez et al*., 2003; *Zeidberg and Robison*, 2007], the area suitable for paralarvae development to maturity might be expanding poleward.

Despite the accepted general vertical expansion of the hypoxic zone [*Stramma et al*., 2008, 2010], the present observations represent only one sampling window, without any view of the development over time, which makes it difficult to reach firm conclusions about the complex situation in this study area. In the study of *Cepeda-Morales et al*. [2013], stations close to E37 near Cabo Corrientes encountered the oxypleth of 9 μmol/kg at levels deeper than 100 m in a typical March. This observation is consistent with the hypothesis that the oxygenated layer is thinning in recent years, although such sparse information cannot be definitive. The need is clear, therefore, to begin planktonic monitoring in the context of environmental conditions. It is necessary first of all to determine the actual variability and overall rate of reduction of this preferential habitat of the paralarvae of the SD complex and other zooplanktonic groups. Documenting the effects of a vertically shrinking habitat, in combination with warming related to climate change and during ENSO events, on the paralarvae and the coastal demersal and pelagic fish species with affinity to the oxygenated water, such as described by *Davies et al*. [2015], would provide valuable indicators of the changes in the pelagic ecosystem related to the expansion of the OMZs.

Acknowledgments

This work was made possible thanks to the financial support of SEP-CONACyT (contracts 2014-236864) and by the Instituto Politécnico Nacional (Multidisciplinary Project 2015-0176). The hydrographic and biological data used for this paper are available on request by writing to L. Sanchez-Velastco (lsvelasc@gmail.com) and E. Beier (ebeier@cicese.mx). We particularly acknowledge the contribution of the late Miguel Fernando Lavín Peregrina (CICESE), without whose contribution and encouragement, this work would not have been possible. Cruiser Designer, CHL maps and ImSatO© 2015, CICESE, Carlos Cabrera, All rights reserved. E.B., V.G., and L.S.V. also participated in the CONACyT project (SEP-2011-168034-T). The altimeter product was produced by Ssalto/Duacs and distributed by AVISO, with support from CNES. We thank the scientific and technical staff who took part in the cruise aboard the R/V Francisco de Ulloa. J. G. Avalos-Díaz helped with genetic analysis. Special thanks to Editor P. G. Brewer and the two anonymous referees for helping improve this article.

References

Aljanabi, S. M., and I. Martinez (1997), Universal and rapid salt-extraction of high quality genomic DNA for PCR-based techniques, *Nucleic Acids Res.*, *25*(22), 4692–4693.

Argüelles, J., P. Rodhouse, P. Villegas, and G. Castillo (2001), Age, growth and population structure of the jumbo flying squid *Dosidicus gigas* in Peruvian waters, *Fish. Res.*, *54*(1), 51–61.

Aristegui, J., and M. F. Montero (2005), Temporal and spatial changes in plankton respiration and biomass in the Canary Islands region: The effect of mesoscale variability, *J. Mar. Syst.*, *54*(1–4), 65–82, doi:10.1016/j.jmarsys.2004.07.004.

Aristegui, J., P. Tett, A. Hernández-Guerra, G. Basterretxea, M. F. Montero, K. Wild, P. Sangrá, S. Hernández-León, M. Canton, and J. Garcia-Braun (1997), The influence of island-generated eddies on chlorophyll distribution: A study of mesoscale variation around Gran Canaria, *Deep Sea Res., Part I*, *44*(1), 71–96.

Baltar, F., J. Arístegui, M. F. Montero, M. Espino, J. M. Gasol, and G. J. Herndl (2009), Mesoscale variability modulates seasonal changes in the trophic structure of nano-and picoplankton communities across the NW Africa-Canary Islands transition zone, *Prog. Oceanogr.*, *83*(1), 180–188.

Bazzino, G., E. Rivera Arriaga, I. Azuz-Adeath, L. Alpuche Gual, and G. Villalobos Zapata (2010), Calamar gigante (*Dosidicus gigas*) y cambio climático: Adaptaciones y vulnerabilidad, in *Cambio climático en México un Enfoque Costero y Marino*, pp. 473–482, Univ. Autónoma de Campeche, Campeche, Mexico.

Beers, J. R. (1976), Determination of zooplankton biomass, in *Zooplankton Fixation and Preservation*, edited by H. F. Steedman, pp. 35–84, UNESCO, Paris.

Camarillo-Coop, S., C. A. Salinas-Zavala, M. Manzano-Sarabia, and E. A. Aragón-Noriega (2011), Presence of *Dosidicus gigas* paralarvae (Cephalopoda: Ommastrephidae) in the central Gulf of California, Mexico related to oceanographic conditions, *J. Mar. Biol. Assoc. U. K.*, *91*(04), 807–814.

Cepeda-Morales, J., G. Gaxiola-Castro, E. Beier, and V. M. Godínez (2013), The mechanisms involved in defining the northern boundary of the shallow oxygen minimum zone in the eastern tropical Pacific Ocean off Mexico, *Deep Sea Res., Part I*, *76*, 1–12, doi:10.1016/j.dsr.2013.02.004.

Chaigneau, A., M. Le Texier, G. Eldin, C. Grados, and O. Pizarro (2011), Vertical structure of mesoscale eddies in the eastern South Pacific Ocean: A composite analysis from altimetry and Argo profiling floats, *J. Geophys. Res.*, *116*, C11025, doi:10.1029/2011JC007134.

Chavez, F. P., J. Ryan, S. E. Lluch-Cota, and M. Ñiquen C. (2003), From Anchovies to Sardines and Back: Multidecadal Change in the Pacific Ocean, *Science*, *299*(5604), 217–221, doi:10.1126/science.1075880.

Clark, E., and D. R. Nelson (1997), Young whale sharks, *Rhincodon typus*, feeding on copepod bloom near La Paz, México, *Environ. Biol. Fish.*, *50*, 63–73.

Collins, C. A., R. Castro, and A. S. Mascarenhas Jr. (2014), Properties of an upper ocean front associated with water mass boundaries at the entrance to the Gulf of California, November 2004, *Deep Sea Res., Part II*, *119*, 48–60, doi:10.1016/j.dsr2.2014.06.002.

Danell-Jiménez, A., L. Sánchez-Velasco, M. F. Lavín, and S. G. Marinone (2009), Three-dimensional distribution of larval fish assemblages across a surface thermal/chlorophyll front in a semienclosed sea, *Estuarine Coastal Shelf Sci.*, *85*(3), 487–496.

Daniel, W. W. (2008), *Biostatistics: A foundation for analysis in health sciences*, John Wiley, Hoboken, USA.

Davies, S. M., L. Sánchez-Velasco, E. Beier, V. M. Godínez, E. D. Barton, and A. Tamayo (2015), Three-dimensional distribution of larval fish habitats in the shallow oxygen minimum zone in the eastern tropical Pacific Ocean off Mexico, *Deep Sea Res., Part I*, *101*, 118–129, doi:10.1016/j.dsr.2015.04.003.

De Silva-Dávila, R., C. Franco Gordo, F. G. Hochberg, E. Godínez Domínguez, R. Avendaño-Ibarra, J. Gómez-Gutiérrez, and C. J. Robinson (2015), Cephalopod paralarval assemblages in the Gulf of California during 2004–2007, *Mar. Ecol. Prog. Ser.*, *520*, 123–141, doi:10.3354/meps11074.

Diaz, R. J., and R. Rosenberg (2008), Spreading dead zones and consequences for marine ecosystems, *Science*, *321*(5891), 926–929.

Ducet, N., P.-Y. Le Traon, and G. Reverdin (2000), Global high-resolution mapping of ocean circulation from TOPEX/Poseidon and ERS-1 and-2, *J. Geophys. Res.*, *105*(C8), 19,477–19,498.

Ehrhardt, N., P. Jacquemin, B. Garcia, D. Gonzalez, B. Lopez, C. Ortiz, and N. Solis (1983), On the fishery and biology of the giant squid *Dosidicus gigas* in the Gulf of California, Mexico, *Fish. Tech. Pap. 231*, FAO, Rome.

Fernández-Álamo, M. A., and J. Färber-Lorda (2006), Zooplankton and the oceanography of the eastern tropical Pacific: A review, *Prog. Oceanogr.*, *69*(2–4), 318–359, doi:10.1016/j.pocean.2006.03.008.

Fiedler, P. C., and L. D. Talley (2006), Hydrography of the eastern tropical Pacific: A review, *Prog. Oceanogr.*, *69*(2–4), 143–180, doi:10.1016/j.pocean.2006.03.008.

Fiedler, P. C., F. P. Chavez, D. W. Behringer, and S. B. Reilly (1992), Physical and biological effects of Los Ninos in the eastern tropical Pacific, 1986–1989, *Deep Sea Res., Part A*, *39*(2), 199–219.

Gilly, W. F., C. A. Elliger, C. A. Salinas, S. Camarilla-Coop, G. Bazzino, and M. Beman (2006), Spawning by jumbo squid *Dosidicus gigas* in San Pedro Mártir Basin, Gulf of California, Mexico, *Mar. Ecol. Prog. Ser.*, *313*, 125–133.

Gilly, W. F., J. M. Beman, S. Y. Litvin, and B. H. Robison (2013), Oceanographic and biological effects of shoaling of the oxygen minimum zone, *Annu. Rev. Mar. Sci.*, *5*, 393–420.

Godínez, V. M., E. Beier, M. F. Lavín, and J. A. Kurczyn (2010), Circulation at the entrance of the Gulf of California from satellite altimeter and hydrographic observations, *J. Geophys. Res.*, *115*, C04007, doi:10.1029/2009JC005705.

Godínez, V. M., M. F. Lavín, L. Sánchez-Velasco, D. U. Hernández-Becerril, and C. Cabrera-Ramos (2011), Datos hidrográficos en el Golfo de California: Campaña GOLCA-1107 (27 de julio al 4 de agosto del 2011), *Informe Téc. 102304*, Dep. de Oceanogr. Física, CICESE, Ensenada, México. [Available at http://oceanografia.cicese.mx/reportes/2011/.]

Godínez, V. M., M. F. Lavín, L. Sánchez-Velasco, and C. E. Cabrera-Ramos (2012), Datos hidrográficos en el Golfo de California: Campaña GOLCA-1204 (26 de abril al 4 de mayo del 2012), *Informe Téc. 104573*, Dep. de Oceanogr. Física, CICESE, Ensenada, México. [Available at http://oceanografia.cicese.mx/2012/.]

Graves, L. P., J. C. McWilliams, and M. T. Montgomery (2006), Vortex evolution due to straining: A mechanism for dominance of strong, interior anticyclones, *Geophys. Astrophys. Fluid Dyn.*, *100*(3), 151–183.

Gray, J. S., S. W. Rudolfi, and Y. O. Ying (2002), Effects of hypoxia and organic enrichment on the coastal marine environment, *Mar. Ecol. Prog. Ser.*, *238*, 249–279.

Hoving, H. J., W. F. Gilly, U. Markaida, K. J. Bernoit-Bird, Z. W. Brown, P. Daniel, J. C. Field, L. Parassenti, B. Liu, and B. Campos (2013), Extreme plasticity in life-history strategy allows a migratory predator (jumbo squid) to cope with changing climate, *Global Change Biology*, *19*, 2089–2103, doi:10.1111/gcb.12198.

Hofmann, F., E. T. Peltzer, P. M. Walz, and P. G. Brewer (2011), Hypoxia by degrees: Establishing definitions for a changing ocean, *Deep Sea Res., Part I*, *58*(12), 1212–1226, doi:10.1016/j.dsr.2011.09.004.

Hofmann, F., E. T. Peltzer, and P. G. Brewer (2012), Kinetic bottlenecks to chemical exchange rates for deep-sea animals—Part 1: Oxygen, *Biogeosciences*, *9*, 13,817–13,856, doi:10.5194/bgd-9-13817-2012.

IOC, SCOR, and IAPSO (2010), The international thermodynamic equation of seawater—2010: Calculation and use of thermodynamic properties, in *Intergovernmental Oceanographic Commission, Manuals and Guides 56*, 196 pp., Paris, France, UNESCO.

Kimura, M. (1980), A simple method for estimating evolutionary rates of base substitutions through comparative studies of nucleotide sequences, *J. Mol. Evol.*, *16*(2), 111–120.

Kiyofuji, H., and S.-I. Saitoh (2004), Use of nighttime visible images to detect Japanese common squid Todarodes pacificus fishing areas and potential migration routes in the Sea of Japan, *Mar. Ecol. Prog. Ser.*, *276*, 173–186.

Klein, P., and G. Lapeyre (2009), The oceanic vertical pump induced by mesoscale and submesoscale turbulence, *Annu. Rev. Mar. Sci.*, *1*, 351–375.

Kramer, D., M. J. Kalin, E. G. Stevens, J. R. Thrailkill, and J. R. Zweifel (1972), Collection and processing data on fish eggs and larvae in the California Current region, *NOAA Tech. Rep. NMFS CIRC-370*, pp. 1–38, National Marine Fisheries Service, La Jolla, USA.

Kurczyn, J. A., E. Beier, M. F. Lavín, and A. Chaigneau (2012), Mesoscale eddies in the northeastern Pacific tropical-subtropical transition zone: Statistical characterization from satellite altimetry, *J. Geophys. Res.*, *117*, C10021, doi:10.1029/2012JC007970.

Kurczyn, J. A., E. Beier, M. F. Lavín, A. Chaigneau, and V. M. Godínez (2013), Anatomy and evolution of a cyclonic mesoscale eddy observed in the northeastern Pacific tropical-subtropical transition zone, *J. Geophys. Res. Oceans*, *118*, 5931–5950, doi:10.1002/2013JC009339.

Lavín, M. F., E. Beier, J. Gómez-Valdés, V. M. Godínez, and J. García (2006), On the summer poleward coastal current off SW México, *Geophys. Res. Lett.*, *33*, L02601, doi:10.1029/2005GL024686.
León-Chávez, C. A., L. Sanchez-Velasco, E. Beier, M. F. Lavín, V. M. Godínez, and J. Färber-Lorda (2010), Larval fish assemblages and circulation in the Eastern Tropical Pacific in Autumn and Winter, *J. Plankton Res.*, *32*(4), 397–410, doi:10.1093/plankt/fbp138.
León-Chávez, C. A., E. Beier, L. Sánchez-Velasco, E. D. Barton, and V. M. Godínez (2015), Role of circulation scales and water mass distributions on larval fish habitats in the Eastern Tropical Pacific off Mexico, *J. Geophys. Res. Oceans*, *120*, 3987–4002, doi:10.1002/2014JC010289.
Le Traon, P., Y. Faugere, F. Hernandez, J. Dorandeu, F. Mertz, and M. Ablain (2003), Can we merge GEOSAT Follow-On with TOPEX/POSEIDON and ERS-2 for an improved description of the ocean circulation?, *J. Atmos. Oceanic Technol.*, *20*(6), 889–895.
Lynch, M. (1977), Zooplankton competition and plankton community structure, *Limnol. Oceanogr.*, 4(*22*),775–777, doi:10.4319/lo.1977.22.4.0775.
Mahadevan, A., L. N. Thomas, and A. Tandon (2008), Comment on "Eddy/Wind Interactions Stimulate Extraordinary Mid-Ocean Plankton Blooms", *Science*, *320*(5875), 448–448.
Markaida, U. (2006), Population structure and reproductive biology of jumbo squid *Dosidicus gigas* from the Gulf of California after the 1997–1998 El Niño event, *Fish. Res.*, *79*(1), 28–37.
Markaida, U., and O. Sosa-Nishizaki (2001), Reproductive biology of jumbo squid Dosidicus gigas in the Gulf of California, 1995–1997, *Fish. Res.*, *54*(1), 63–82.
Markaida, U., J. J. Rosenthal, and W. F. Gilly (2005), Tagging studies on the jumbo squid (*Dosidicus gigas*) in the Gulf of California, Mexico, *Fish. Bull.*, *103*(1), 219–226.
Martin, A. P., and K. J. Richards (2001), Mechanisms for vertical nutrient transport within a North Atlantic mesoscale eddy, *Deep Sea Res., Part II*, *48*(4–5), 757–773.
McGillicuddy, D., A. Robinson, D. Siegel, H. Jannasch, R. Johnson, T. Dickey, J. McNeil, A. Michaels, and A. Knap (1998), Influence of mesoscale eddies on new production in the Sargasso Sea, *Nature*, *394*(6690), 263–266.
McGillicuddy, D. J., et al. (2007), Eddy/Wind interactions stimulate extraordinary mid-ocean plankton blooms, *Science*, *316*(5827), 1021–1026, doi:10.1126/science.1136256.
Nigmatullin, C. M., K. Nesis, and A. Arkhipkin (2001), A review of the biology of the jumbo squid Dosidicus gigas (Cephalopoda: Ommastrephidae), *Fish. Res.*, *54*(1), 9–19.
Pawlowicz, R., D. G. Wright, and F. J. Millero (2010), The effects of biogeochemical processes on oceanic conductivity/salinity/density relationships and the characterization of real seawater, *Ocean Sci.*, *7*, 773–836.
Prince, E. D., and C. P. Goodyear (2006), Hypoxia-based habitat compression of tropical pelagic fishes, *Fish. Oceanogr.*, *15*(6), 451–464.
Ramos-Castillejos, J. E., C. A. Salinas-Zavala, S. Camarillo-Coop, and L. M. Enríquez-Paredes (2010), Paralarvae of the jumbo squid, Dosidicus gigas, *Invertebrate Biol.*, *129*(2), 172–183.
Robinson, C. J., J. Gómez-Gutierrez, U. Markaida, and W. F. GIlly (2015), Prolonged decline of jumbo squid (*Dosidicus gigas*) landing in the Gulf of California associated with chronically low wind stress and decreased chlorophyll a after EL Niño 2009-2010, *Fish. Res.*, *173*, 128–138, doi:10.1016/j.fishres.2015.08.014.
Rohner, C. A., S. J. Pierce, A. D. Marshal, S. J. Weeks, M. B. Bennett, and A. J. Richardson (2013), Trends in sightings and environmental influences on coastal aggregation of manta rays and whale sharks, *Mar. Ecol. Prog. Ser.*, *482*, 153–168.
Rosa, R., and B. A. Seibel (2010), Metabolic physiology of the Humboldt squid, *Dosidicus gigas*: Implications for vertical migration in a pronounced oxygen minimum zone, *Prog. Oceanogr.*, *86*, 72–80.
Sánchez-Velasco, L., M. F. Lavín, S. P. A. Jiménez-Rosenberg, V. M. Godínez, E. Santamaría-del-Ángel, and D. U. Hernández-Becerril (2013), Three-dimensional distribution of fish larvae in a cyclonic Eddy in the Gulf of California during the summer, *Deep Sea Res., Part I*, *175*, 39–51.
Sangrá, P., J. Pelegrí, A. Hernández-Guerra, I. Arregui, J. Martin, A. Marrero-Díaz, A. Martinez, A. Ratsimandresey, and A. Rodríguez-Santana (2005), Life history of an anticyclonic eddy, *J. Geophys. Res.*, *110*, C03021, doi:10.1029/2004JC002526.
Sangrà, P., A. Pascual, Á. Rodríguez-Santana, F. Machín, E. Mason, J. C. McWilliams, J. L. Pelegrí, C. Dong, A. Rubio, and J. Arístegui (2009), The Canary Eddy Corridor: A major pathway for long-lived eddies in the subtropical North Atlantic, *Deep Sea Res., Part I*, *56*(12), 2100–2114.
Siegel, S., and N. J. Castellán (1988), *Non-Parametric Statistics for the Behavioral Sciences, Stat. Ser.*, McGraw-Hill, N. Y.
Smith, P. E., and S. L. Richardson (1979), Tecnicas modelo para prospecciones de huevos y larvas de peces pelágicos, *Doc. Tec. Pesca 175*, FAO, Rome.
Sokal, R. R., and F. J. Rohlf (1985), *Biometry*, Blume, Barcelona, Spain.
Staaf, D., S. Camarillo Coop, S. H. D. Haddock, A. C. Nyack, J. Payne, C. A. Salinas Zavala, B. A. Seibel, L. Trueblood, C. Widmer, and W. F. Gilly (2008), Natural egg mass deposition by the Humboldt squid (*Dosidicus gigas*) in the Gulf of California and characteristics of hatchlings and paralarvae, *J. Mar. Biol. Assoc. U. K.*, *88*(4), 759–770, doi:10.1017/S0025315408001422.
Staaf, D., L. D. Zeidberg, and W. F. Gilly (2011), Effects of temperature on embryonic development of the Humboldt squid *Dosidicus gigas*, *Mar. Ecol. Prog. Ser.*, *441*, 165–175, doi:10.3354/meps09389.
Staaf, D. J., J. V. Redfern, W. F. Gilly, W. Watson, and L. T. Ballance (2013), Distribution of ommastrephid paralarvae in the eastern tropical Pacific, *Fish. Bull.*, *111*(1), 78–89.
Stewart, J. S., J. C. Field, U. Markaida, and W. F. Gilly (2013), Behavioral ecology of jumbo squid (*Dosidicus gigas*) in relation to oxygen minimum zones, *Deep Sea Res., Part II*, *95*, 197–208.
Stramma, L., G. C. Johnson, J. Sprintall, and V. Mohrholz (2008), Expanding oxygen-minimum zones in the tropical oceans, *Science*, *320*(5876), 655–658, doi:10.1126/science.1153847.
Stramma, L., S. Schmidtko, L. A. Levin, and G. C. Johnson (2010), Ocean oxygen minima expansions and their biological impacts, *Deep Sea Res., Part I*, *57*(4), 587–595, doi:10.1016/j.dsr.2010.01.005.
Tamura, K., G. Stecher, D. Peterson, A. Filipski, and S. Kumar (2013), MEGA6: Molecular evolutionary genetics analysis version 6.0, *Mol. Biol. Evol.*, *30*(12), 2725–2729.
Thurnherr, A. (2010), A practical assessment of the errors associated with full-depth LADCP profiles obtained using Teledyne RDI Workhorse acoustic Doppler current profilers, *J. Atmos. Oceanic Technol.*, *27*(7), 1215–1227.
Ueynagi, S., and H. Nonaka (1993), Distribution of ommastrephid paralarvae in the central eastern Pacific Ocean, in *Recent Advances in Cephalopod Fisheries Biology*, edited by T. Okutani, R. K. O'Dor, and T. Kubodera, pp. 587–589, Tokai University Press, Tokyo, Japan.
Vecchione, M. (1999), Extraordinary abundance of squid paralarvae in the tropical eastern Pacific Ocean during El Niño of 1987, *Fish. Bull.*, *97*(4), 1025–1030.

Visbeck, M. (2002), Deep velocity profiling using lowered acoustic doppler current profilers: Bottom track and inverse solutions, *J. Atmos. Oceanic Technol.*, *19*(5), 794–807.

Wormuth, J. H., R. K. O'Dor, N. Balch, M. C. Dunning, E. C. Forch, R. F. Harman, and T. W. Rowell (1992), Familly Ommastrephidae, in, *Larval and juvenile cephalopods: A manual for their identification, Smithsonian contributions to zoology, No. 513*, edited by Sweeny et al., pp. 105–121, Smithsonian Institution Press, Wash.

Yoo, L., J. Hae-Kyun, J. Yamamoto, S. Tomonori, and Y. Sakurai (2014), Laboratory observations on the vertical swimming behavior of Japanese common squid *Todarodes pacificus* paralarvae as they ascend into warm surface waters, *Fish. Sci.*, *80*, 925–932, doi:10.1007/s12562-014-0767-1.

Zeidberg, L. D., and B. H. Robison (2007), Invasive range expansion by the Humboldt squid, Dosidicus gigas, in the eastern North Pacific, *Proc. Natl. Acad. Sci. U. S. A.*, *104*(31), 12,948–12,950.